Hindawi Publishing Corporation
Science and Technology of Nuclear Installations
Volume 2016, Article ID 9012747, 12 pages
http://dx.doi.org/10.1155/2016/9012747

Research Article

Design, Construction, and Modeling of a ^{252}Cf Neutron Irradiator

Blake C. Anderson, Keith E. Holbert, and Herbert Bowler

Arizona State University, Tempe, AZ 85287-5706, USA

Correspondence should be addressed to Keith E. Holbert; holbert@asu.edu

Received 1 June 2016; Revised 27 July 2016; Accepted 31 July 2016

Academic Editor: Alejandro Clausse

Neutron production methods are an integral part of research and analysis for an array of applications. This paper examines methods of neutron production, and the advantages of constructing a radioisotopic neutron irradiator assembly using ^{252}Cf. Characteristic neutron behavior and cost-benefit comparative analysis between alternative modes of neutron production are also examined. The irradiator is described from initial conception to the finished design. MCNP modeling shows a total neutron flux of 3×10^5 n/(cm^2·s) in the irradiation chamber for a 25 μg source. Measurements of the gamma-ray and neutron dose rates near the external surface of the irradiator assembly are 120 μGy/h and 30 μSv/h, respectively, during irradiation. At completion of the project, total material, and labor costs remained below $50,000.

1. Introduction

Neutrons are useful in a variety of applications, spanning from laboratory investigations and field measurements, to national security and medical treatment. The manner by which neutrons are generated determines the particular energies and spectrum of the resulting emissions. Many studies exist on irradiators; however, most of the literature is rather dated. This paper seeks to modernize information on the design, construction, and modeling of a ^{252}Cf neutron irradiator and provide a starting foundation to benefit others who might undertake such an endeavor.

Neutron irradiators are often employed in materials research, utilizing various techniques and methods such as neutron activation analysis (NAA), neutron radiography, and neutron diffraction for elemental analyses. Activation products can be measured using a high-purity germanium detector with gamma spectroscopy analysis software [1]. NAA is frequently employed by professionals from several different disciplines, for example, biomedical, chemical, and petrochemical, for purposes such as oil well logging and identification of trace elements in samples [1]. Diffraction methods can be used to determine the moisture and hydrocarbon concentrations of hydrogen-rich samples [2]. Fundamental concepts in nuclear physics may be taught to students by employing a neutron howitzer for irradiation experiments. A neutron howitzer is a specialized irradiator in which the sample to be exposed is dropped down into a tube. For example, ^{239}Pu has been produced by students from irradiating natural uranium within a neutron howitzer [3].

This paper is organized as follows. Section 2 compares neutron sources including their benefits and disadvantages. Section 3 describes the design, construction, and modeling of a ^{252}Cf-based neutron irradiator. Monte Carlo modeling of the facility is detailed in Section 4. Section 5 concludes.

2. Neutron Source Selection

In general, there are three main sources of neutrons: (1) radioisotopes, (2) accelerators, and (3) reactors. The radiological characteristics of each vary greatly in terms of energy, flux, and spectra produced as well as capital and operating costs. Neutrons of particular energies are sought for different purposes. Thermal neutrons used by researchers and industry are excellent for activation of most sample materials, due to matter tending to have higher neutron capture cross sections at lower neutron energy. Epithermal neutrons are desired

Table 1: Comparison of neutron sources.

Neutron source	Production mode	Neutron yield (n/s)	Flux	Average neutron energies (MeV)	Spectrum	Cost ($)
^{241}AmBe	(α, n) [19]	7.0×10^{-5} (per Bq)	Low	3.3, 4.3, 4.9, 6.8, 7.7, 9.5	Continuous	10^4
^{241}AmF		4.0×10^{-6} (per Bq)		1.8, 2.1		
^{241}AmB		1.4×10^{-5} (per Bq)		2.6		
^{239}PuBe [2]		3.8×10^{-5} (per Bq)		~3.3		
D-D generator [20]	D(d, n)	10^6–10^{11}	Moderate	2.45	Monoenergetic	10^5
D-T generator [20]	T(d, n)	10^8–5×10^{13}		14.1		
^{252}Cf [21]	Spontaneous fission	1.2×10^{-1} (per Bq)	Low	2.0	Fission	10^4
Research reactor [12]	Fission	$>10^{16}$	High			$>10^8$ [7]

in the medical field for boron neutron capture therapy [4]. Neutrons of all energies are needed for uses in radiobiological research and radiotherapy and are attained by various sources and setups [4]. Table 1 compares radiological characteristics of common neutron sources, including mode of neutron production, yield, flux, mean energy of emission, neutron spectrum, and relative cost.

The emitted neutrons may be focused into a beam for activation experiments, regardless of the neutron source. This neutron streaming is accomplished by surrounding the source location with reflecting or moderating material and leaving an empty pathway for the neutrons to propagate through freely (minimal interactions), with the volume along the path having a higher flux due to the scattering effects induced by the peripheral materials.

2.1. Nuclear Reactors. The purpose of a research reactor is to produce and sustain nuclear fission for experimentation with high neutron fluxes preferred, rather than electric power production. In the late 1950s, the Atomic Energy Commission (AEC) financially supported the construction of research reactors at universities in the United States. Many of these were Training Research Isotope-General Atomics (TRIGA) reactors. For almost 60 years, TRIGA reactor popularity among North American universities has helped to support the peaceful applications of nuclear technology [5]. Figure 1 shows that the number of operational research reactors at US universities grew upwards to 50+ by the midseventies and has since followed a declining trend down to the remaining 24 research reactors operating today. Murray collected and compiled data showing a correlation between university reactor usage and power output. Not surprisingly, he found that the reactors producing the highest fluxes were the most used among faculty researchers [6]. Bernard and Hu believe university reactors have been neglected by their faculty and staff, who consistently look elsewhere for the highest flux-producing reactors for their experiments and research. Universities with research reactors generally have a difficult time accruing funds to pay for both professional engineering staff and upgrading old or obsolete equipment with updated,

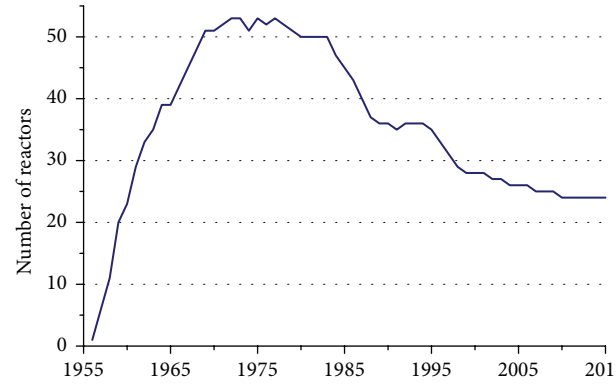

Figure 1: Nuclear Regulatory Commission licensed research reactors at US universities (does not include those at industrial and other government sites such as Department of Energy national laboratories); data are compiled from multiple volumes of [11].

state-of-the-art instruments. This lack of sufficient funds leads researchers to conduct studies at places like the national laboratories where time can be purchased to utilize cutting-edge nuclear facilities with full-time technical staff [7, 8]. In contrast, some countries, like Jordan, currently have plans for the construction and commissioning of research reactors [9]. According to the International Atomic Energy Agency, there are eight research reactors under construction and ten planned as of May 2016—only one of which is in the US [10].

The TRIGA design serves as a comparative example for the other neutron sources examined in this paper. Several updates to the TRIGA reactor design have occurred and demonstrate a wide range of research capabilities and radiological characteristics. TRIGA reactors provide a regional compartment of high flux where material sample activation near the reactor core can be carried out. The characterized spectrum of neutrons in this irradiating region varies with the different TRIGA models owned by various organizations. For instance, the U.S. Geological Survey operates a 1 MW TRIGA capable of producing a *thermal* neutron flux of approximately 2.01×10^{13} n/(cm^2·s), experimentally determined using gold

foils. Theoretically however, a MCNP5 model determined that a *total* flux of up to 4.51×10^{13} n/(cm^2·s) is possible [12].

Commissioning a new nuclear research reactor requires considerable capital expenditure and extensive planning. This is a long-term commitment by an institution which assumes all responsibilities including financial requirements far into the future. A conservative estimate of over $200 million in capital is required for commissioning a basic research reactor, before factoring in many other significant costs such as the buildings and licensing [7]. With that said, it is still highly desirable to have an operational research reactor on site or nearby for both researchers and local industries. The investment, although sizable, may be justifiable considering the long-term benefit to the institution. Research reactors are highly desirable due to the fission spectrum of neutron energies at the highest fluxes available among the neutron sources.

2.2. Accelerators. Recently, accelerator-based systems seem to be receiving more interest than reactors for providing a high neutron flux. However, accelerators generate monoenergetic neutrons which limits the range of applicability for a multitude of research areas. Advantages of accelerators include selectivity and control of particular monoenergetic neutron energies and fluxes as well as the option to relocate the source and cost several orders of magnitude less than that of a research reactor. Accelerators require higher capital compared to radioisotopic neutron sources and are less portable than the isotopic-based irradiators, requiring extensive dismantling and reassembly in order to transport between locations; generally, accelerators are stationary structures.

Conventional accelerators utilize a D-D or D-T nuclear reaction to generate neutrons. Deuteron cations, required for both reactions, are produced in a radiofrequency ion source and are accelerated to high energy. A focused beam of accelerated deuterons collides with one of two titanium compound targets, TiD or TiT, determining the energy of the neutrons ejected. The nuclear reaction, D(d, n)^{3}He, generates monoenergetic neutrons of 2.45 MeV and is induced by bombarding titanium-deuterium (TiD) with accelerated deuteron ions. This is the more economical choice between the two target material options. For Sinha et al., the maximum attained neutron yield for their accelerator using the D-D reaction was 10^8 n/s [13]. The deuterons were accelerated to energies between 0 and 300 keV to induce the TiD target interaction. Alternatively, a greater neutron beam energy (14.1 MeV) can be achieved by utilizing the titanium-tritium (TiT) target. A T(d, n)^{4}He reaction from bombarding TiT with accelerated deuteron cations can generate considerable neutron yields of 5×10^{13} n/s and greater. One drawback of tritiated targets for deuteron reactions, however, is their higher price and therefore cost, to operate [14]. Furthermore, most neutron generators have a finite lifetime.

2.3. Radioisotopes. Radioisotopic sources have many benefits that include easy transportability, low relative cost, zero to little maintenance, and no external power requirements. Radioisotopic-produced neutrons are generated by any of three primary modes of energy decay: (1) (α, n) reaction, (2) (γ, n) reaction, and (3) spontaneous fission (SF) [15]. The intensity of neutrons produced in neutron emission reactions is determined by the half-life of the particular emitter in the source compound [16].

The neutron energy spectrum, emitted by sources like ^{241}AmBe or that of PuBe, is determined by the alpha emission energy contributed in the (α, n) reaction. Since the α-decay emits doubly charged helium nuclei, coulombic repulsion can be minimized by using compound sources consisting of light elements. Photoneutron sources relying on the (γ, n) reaction yield monoenergetic neutrons rather than a spectrum of varying energies and are coupled with additional gamma emission. Both (α, n) and (γ, n) reactions can be generally labeled as neutron emission reactions. Distinctly different from the first two isotopic neutron sources are SF radioisotopes. SF sources emit a fission neutron spectrum, characteristic of nuclear reactor spectra.

2.3.1. AmBe. The neutron yield of a ^{241}AmBe source depends on the composition and volume of the AmO_2 and ^{9}Be used to make up a sealed neutron source. ^{241}AmBe users benefit from an exceptionally stable flux over many years owed to its long half-life. Comparatively, ^{241}AmBe incurs a smaller expenditure among the radioisotope sources. However, the neutron flux is also smaller than the other sources. This is disadvantageous when large samples need to be activated since the radiation intensity will be disproportionate closest to the source, as the sample periphery becomes activated at a slower rate than the parts of the sample closest to the source. An important property of ^{241}AmBe is its high ratio of *thermal* neutrons in its characteristic spectrum, compared to that of other radioisotopic sources [17].

2.3.2. PuBe. Inexpensive neutron sources like PuBe have been utilized frequently in the petroleum industry for oil well logging and calibrating measuring instruments. $PuBe_{13}$ is a single face centered cubic structure synthesized from pure ^{239}Pu metal (oxide) and beryllium. This neutron source has certain advantages over similar (α, n) reaction sources such as ^{241}AmBe and AmLi. A desirable property of a PuBe source is its comparatively lower gamma intensity, coupled with its neutron emission, as compared to the other alpha-decay sources. Therefore, PuBe is favorable for situations desiring little to no gamma interactions during sample activation experiments. Like ^{241}AmBe, PuBe has a stable neutron yield and does not need to be replenished often [18]. Although PuBe has desirable properties as a neutron source, its use has been in decline in recent years due to the inherent need for plutonium.

2.3.3. Californium. Like most of the radioisotopes discussed, ^{252}Cf produces both neutrons and gamma rays among other radiations. With an overall half-life of 2.645 y, ^{252}Cf decays primarily by alpha emission with only 3% of the nuclear transformations being spontaneous fission (SF). This Cf_2O_3 SF source is currently produced by only two facilities in the world, Oak Ridge National Laboratory in the US and

Table 2: ^{252}Cf decay characteristics.

Parameter	Value
Half-life (effective: α and SF)	2.645 y
Half-life (spontaneous fission)	85.5 y
Decay mode	α (96.91%), SF (3.09%)
Alpha energies	6.076 and 6.118 MeV

the Research Institute of Atomic Reactors in Dimitrovgrad, Russia. Cermet wire is formed by the suspension of the metal-oxide compound in a palladium matrix. The wire is encased in a palladium tube and then doubly-encapsulated in an additional stainless steel tube. The typical composition of the oxide source is as follows: 2 weight percent (w/o) of ^{249}Cf, 15 w/o of ^{250}Cf, 4 w/o of ^{251}Cf, and 79 w/o of ^{252}Cf [22]. It is produced in micro quantities by subjugating plutonium to large neutron fluxes on the order of 10^{21} n/(cm^2·s) and larger [23]. Additional decay characteristics of ^{252}Cf are given in Table 2.

Accelerator sources were the most common neutron source available in the mid-1980s when the high initial cost to transmute plutonium into ^{252}Cf prevented many from purchasing this SF source [14]. Magnusson et al. have concluded that irradiated plutonium is composed almost entirely of transcurium elements including all of the berkelium and californium isotopes, requiring complex chemical separation techniques to recover the desired products [23]. This more than likely contributed to the high purchasing price of ^{252}Cf as well as large demand for limited quantities of the isotope, split between industrial, medical, and research fields. Recently however, ^{252}Cf has greatly lowered in price due to advancements in isotope production and separation methods. Typical accelerators can cost upwards of hundreds of thousands of US dollars while ^{252}Cf has declined in cost considerably, to the tens of thousands of dollars range for microgram quantities.

2.4. Existing Neutron Irradiators. Having made these comparisons, our inclination was to use the spontaneous fission ^{252}Cf source. Our primary intended use was to induce low-levels of radioactivity (neutron activation) in small material samples. In a similar application, the University of Minnesota built a neutron irradiation apparatus using a borrowed 11.5 mg ^{252}Cf source to test the radiation hardness of photodiodes and other electronic components [24]. The Cf source was obtained under the Californium Industrial Loan Program, which no longer exists.

With the ^{252}Cf source chosen, the potential irradiator characteristics were examined. First and foremost, the irradiator apparatus needed to incorporate passively safe design aspects. The irradiator was intended to be simple in operation and durable over time under heavy use. To that end, several existing irradiators were analyzed for design exemplars as well as individual strengths and weaknesses to improve upon. Although the purposes of the irradiators researched differ, they all utilize a radioisotopic-based neutron source within a structure of moderating and shielding materials. This is the common theme among various neutron irradiators and howitzers.

One example of an education-oriented neutron irradiator is the cylindrical Plexiglas, water moderated, "Visiflux" neutron howitzer, designed by ATOMIC Accessories, Inc. That howitzer was constructed for a university laboratory as an additional resource for teaching radiochemistry, nuclear engineering, and similar disciplines of study. The Visiflux weighs approximately 56.7 kg without water and has a 0.61 m diameter, standing roughly 0.71 m tall. The fully assembled howitzer hosts a neutron source in its center, surrounded by a shield of water. The water shield acts to moderate higher energy neutrons down to thermal equilibrium and helps protect students from the ejected neutrons. The Visiflux handles activities of up to 185 GBq (5 curies), using PoBe or PuBe neutron sources interchangeably [25].

In the past, commercialized neutron irradiators have been designed with parameters to make them appealing to a broad range of potential buyers, but at the cost of a high retail price point. Neutron irradiators can be constructed for a specialized purpose and for a lower cost than that of most commercially available howitzers. Faculty at Arizona State University constructed a neutron howitzer in 1966 for student use in the nuclear physics laboratory. That howitzer is described as a 55-gallon steel barrel, filled with paraffin up to 0.1 m from the top. Wheels affixed to the drum base allowed it to be transported through various laboratories. It did not require substantial shielding, employing a 1 Ci PuBe source, which produced a neutron flux of 3×10^3 n/(cm^2·s). The small flux meant safer operation by students and minimal shielding cost. However, this necessitated increased sample irradiation times to achieve a specified activation level in a material sample. The design of that howitzer was limited to irradiating only basic shapes and small sample sizes. Although Rawls and Voss quoted an exceptionally low cost to make the howitzer, many of the materials used were already owned or donated to the project construction. The funds needed to reconstruct the same irradiator from nothing would actually be significantly higher than stated [26].

Another irradiator described in the literature varied significantly in shape and use compared to the above howitzer. This contrasting irradiator was a dual-hemisphere utilizing a 5 Ci ^{241}AmBe source at its center and constructed specifically for qualitative-quantitative materials analysis. Paraffin wax with 5% being boric acid internally (the dual-hemisphere) and 20% boric acid in the outer components of containment encapsulated the ^{241}AmBe source. Also, lead shielding was arranged around the periphery of the inner paraffin shielding. This helped to provide some attenuation of prompt gamma radiation being emitted from the neutron captures by the borated material [27].

3. Irradiator Design, Construction, and Operation

A setup capable of irradiating small samples was needed in the absence of an onsite nuclear reactor. The ^{252}Cf-based neutron irradiator is primarily fabricated from high density

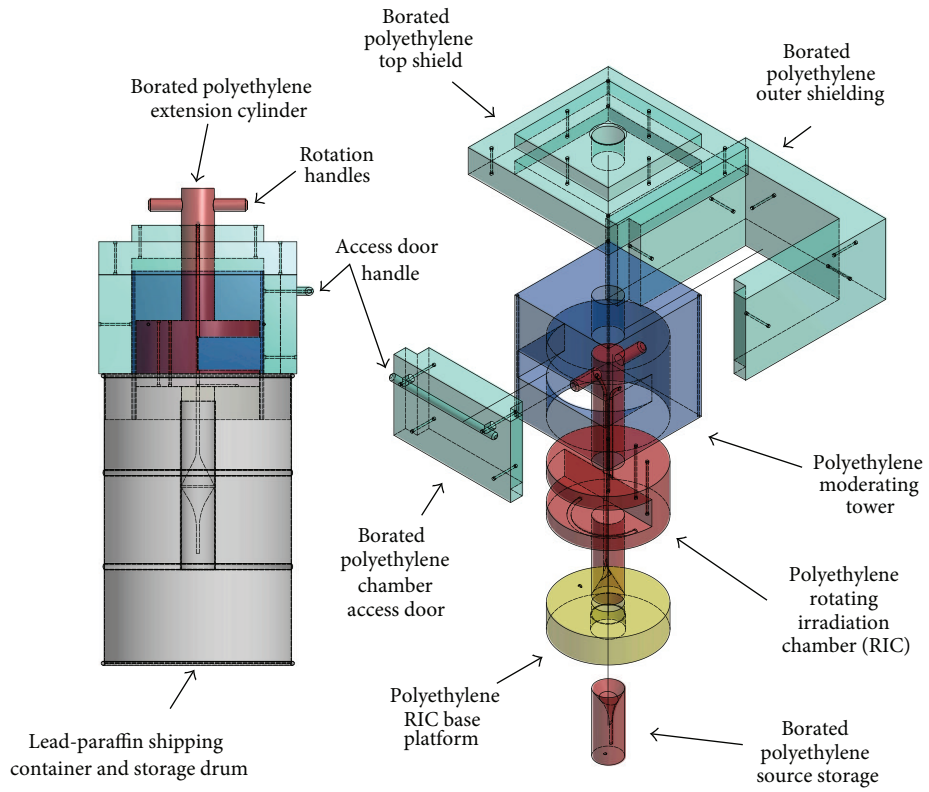

Figure 2: Exploded view irradiator components from computer-aided modeling software.

and purity polyethylene material, as well as interlocking lead bricks. The major components, shown in Figure 2, consist of (1) the shielded neutron source shipping container [black]; (2) the rotating irradiation chamber (RIC) [red]; (3) a donut-shaped polyethylene RIC base [yellow]; (4) a stacked polyethylene moderating tower [blue]; (5) the borated peripheral shielding [cyan]; and (6) a lead wall structure [not shown]. This section describes the design of each component, followed by the assembly of the integrated parts, and ending with the typical operating procedure and measurements of the external radiation emissions.

Table 3: ^{252}Cf source data without moderation.

^{252}Cf mass	25 μg
Neutron emission	5.75×10^7 n/s
Neutron dose at 1 m in air	0.575 mSv/h (57.5 mrem/h)
Neutron energy	2.3 MeV (average)
Gamma exposure at 1 m in air	0.03478 mGy/h (4.0 mR/h)
Gamma energies	0.2–1.8 MeV

3.1. Irradiator Design. The irradiator design had five main goals: (1) to effectively shield operators from neutron and gamma exposure; (2) to use construction materials that diminish unnecessary long-lived activation products (i.e., potential radioactive waste); (3) to increase the neutron flux incident to a sample via neutron moderation; (4) to allow sample size and shape flexibility; and (5) to stay within a predetermined project budget. At the heart of the irradiator is a 2250 cm^3 semicircular shaped compartment within which the sample(s) can be situated. The neutron source is at the radial center of the irradiator, and during irradiation, centered vertically within the sample cavity. This air cavity is part of the RIC, which is composed of high density, pure polyethylene. Surrounding this rotating assembly, housing the irradiation cavity, is the stationary polyethylene-sheet stacked tower. The 40.6 cm × 40.6 cm × 45.7 cm tall tower provides moderation to the chamber, while the periphery is encompassed by layers of borated polyethylene sheets.

Based on the available funds, a 25 μg, 500 MBq (13.4 mCi) ^{252}Cf source was purchased and shipped in a shielded, 55-gallon (208 L) drum. Table 3 gives the unshielded source radiological characteristics. The shipping container was integrated into the irradiator design as the base to reduce costs since it already provided adequate shielding properties for source storage. Cost was lowered further by purchasing commonly manufactured shapes of polyethylene and eliminating the use of custom shaped materials, which are sold at a premium.

The shipping container houses the source internally within a borated polyethylene cylinder at the drum core. The drum itself weighs 230 kg, thus providing a stable base for the rest of the irradiator to be constructed on. The drum acquires

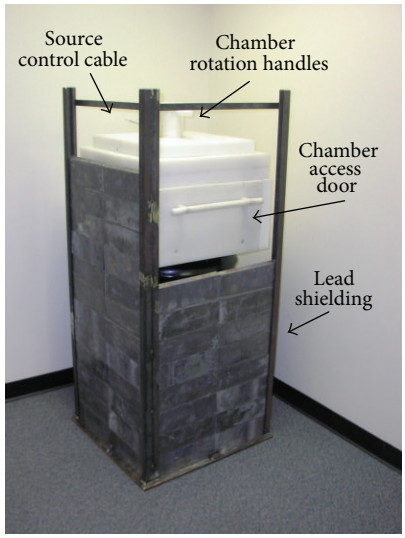

Figure 3: Assembled neutron irradiator with lead shielding.

its shielding properties and weight from being filled with a paraffin-lead mixture. A polyvinyl chloride (PVC) pipe with a 10.2 cm ID (10.8 cm OD) runs vertically through the center of the shipping container. The cylinder housing the source fits snug in the PVC pipe and rests at the bottom of the container core, approximately halfway down the drum. The PVC pipe extrudes from the top surface of the drum by almost the same height as the drum edge (~10 cm).

The source is repositioned between the shipping container core (i.e., the shielded, nonirradiating position) and the irradiating position in the sample chamber, via a control cable. The cable access, located below the rotation grips at the top of the assembly, allows the operator to shift the source vertically. The movement is constrained between the barrel center and the sample chamber ceiling. Two labeled markers affixed to the cable indicate the source location: (1) the vertically centered irradiating position within the sample chamber and (2) the nonirradiating shielded storage position. The cable is confined to the source bore hole, and the source to its two limits at the position maxims (i.e., an inherently safer design constrained by physical size and openings). This means the 3.4 mm diameter stainless steel cable, and hence, source, cannot be accidentally removed from the irradiator due to operator error.

Certainly, operator dose is kept as low as reasonably achievable (ALARA) by limiting their exposure time, following the irradiator operating procedure, and maximizing distance from the irradiating chamber when possible. Furthermore, the design reduces the possibility of radiation streaming. For example, the moderating tower was assembled with horizontally stacked polyethylene (PE) sheets which were then encased with borated PE oriented vertically. Gamma exposure was initially found to exceed 0.15 mSv/h (15 mrem/h) near the irradiator and was addressed by implementing a 5 cm (2 inches) thick lead wall structure surrounding the irradiator assembly. The completed irradiator is shown in Figure 3 and is located at the far corner of a below-grade room.

3.2. Irradiator Construction. This section describes the assembly of the irradiator components in order to better understand its operation. The components themselves were fabricated at the university using machining equipment controlled by our computer-aided drawings. The construction of the overall irradiator is described in the sequence that the components were assembled.

The stationary donut-shaped base, as shown in Figure 4(a), is positioned on the surface of the shipping container. It sits atop the drum and its hollow center fits over the protruding PVC pipe. It provides a platform for the rotating components to slide upon. In particular, it elevates the rotating irradiation chamber (RIC) but remains stationary itself when the RIC is being turned. An aluminum notch protrudes from the top of the donut-shaped platform and provides guidance for the RIC assembly turning. The 38.1 cm diameter RIC rests on the donut-shaped base and includes a drilled out, semicircular track, as shown in Figure 4(b), which limits the RIC assembly rotation to 180°.

The RIC assembly consists of the pure polyethylene irradiation chamber and attached borated cylinders extending below the RIC into the source container, and above to a point of access for rotating the apparatus 180°. The RIC has one bore hole in line with the source. The bore hole runs through the bottom cylindrical extension shown attached in Figure 4(b), through the sample chamber, and through an upper extension (see Figure 2). Another separate but identical bore hole accompanies the source bore hole, except it only runs through the upper extension of the chamber. This latter bore hole allows inserting small wires into the irradiation cavity for providing signals to/from electrical samples. The angled bore hole exit reduces exposure from streaming neutrons that would otherwise have a direct exit route above the chamber. Neutrons are attenuated above and below the source when it is in the irradiating position due to the borated polyethylene construction of the cylindrical extensions from the sample chamber (RIC center). A moderation-increased neutron flux at the sample location is thus achieved while reducing neutron flux outside of the irradiator.

To decrease sample irradiation times, the moderating tower component was utilized. The pure polyethylene used as moderator has a small coefficient of friction and can therefore cause problems with component alignment when assembled. Radial and lateral movement was constricted by the addition of a strong skeletal-like internal frame. The tower internal support is four aluminum rods that run through the corners of the stacked square PE layers. This prevents any wiggle in the horizontal plane and keeps the sides of the moderating tower flush.

The tower is engulfed with no less than 10 cm of borated PE on the periphery. The outer borated PE shield, with a thermal neutron one-tenth thickness of 0.45 inches, has primary responsibility for the overall neutron attenuation and exposure reduction by the irradiator. The periphery of the moderation tower is padded with no less than 10 cm (4 in.) of neutron capturing material. The RIC extensions are constructed of borated material so no gap is created in the outer shielding by the protrusion.

(a) (b)

Figure 4: (a) Stationary donut-shaped component that rests on the shipping drum; (b) bottom of the RIC that rests and slides on the component shown left.

The last component, a lead wall, provides additional protection against high-energy photon exposure. The ^{252}Cf neutron source produces gamma radiation by two mechanisms: (1) direct gamma-ray emission from spontaneous fission and fission product decay and (2) indirect gamma generation from neutron capture events, for example, prompt gamma emission. A steel frame was welded together to support stacked 2-inch thick lead bricks. Use of interlocked lead bricks increases wall stability and significantly reduces gamma-ray streaming through Pb contact points.

3.3. Irradiator Operation. The irradiator may be used by a single operator to perform sample irradiations. Irradiation times vary with sample material and desired activity levels. Scoping calculations are made to estimate a particular sample irradiation time and help assure that no samples become too radioactive, thereby risking unnecessary exposure to the sample handler when removed or exceeding radioactive material license possession limits. The calculations are performed prior to an irradiation, where the *maximum* expected induced activity is estimated from the thermal cross sections for the nuclides within the sample being exposed. The activity of each radionuclide is computed as follows:

$$A = \frac{mN_{\mathrm{A}}\sigma_a\phi}{M}\left[1 - \exp\left(-\frac{\ln(2)\,t}{t_H}\right)\right], \quad (1)$$

where m is the target nuclide mass; N_{A} is Avogadro's number; σ_a is the thermal neutron absorption cross section; ϕ is the neutron flux; M is the nuclide atomic mass; t is the anticipated exposure time; and t_H is the half-life of the activation product.

The sample chamber is accessed only when the source is in the nonirradiating position within the drum, and the lines of sight of the bore holes are disconnected between the drum core and the RIC where the samples are located. This alignment reduces neutron streaming into the sample chamber from the neutron source stored directly below, as well as making the source more difficult to pull up accidentally. The RIC is configured by rotating the handles at the top of the irradiator, as shown in Figure 2, 180° clockwise. A recessed track guides the correct rotation, and a fitting knob does not allow a rotation greater than 180°. The rotation aligns the source bore hole with the stored ^{252}Cf neutron source at the drum core. At this point, the yellow marker on the control cable indicates that the source is recessed. The cable is then pulled out until the red marker is seen at the bore hole exit; this indicates that ^{252}Cf is in the irradiating position in the sample chamber.

For measurement of exposure outside of the irradiator, a Ludlum model 12-4 Bonner sphere-type neutron dose rate meter employing a ^{3}He proportional detector is used. Additionally, gamma radiation exposure from the irradiator and any activated samples are measured using a Ludlum Model 2 survey meter with a detachable Geiger pancake probe (model 44-9). Table 4 shows radiation measurements taken on the borated shield periphery, just under the access door handle.

Table 4: Radiation measurements at the chamber access door.

Source location	Neutron dose rate	Gamma exposure rate
Nonirradiating position (down)	2 μSv/h (0.2 mrem/h)	8 μGy/h (0.9 mR/h)
Irradiation position (up)	42 μSv/h (4.2 mrem/h)	0.15 mGy/h (17 mR/h)

4. MCNP Modeling of the Irradiator

Monte Carlo radiation transport simulations investigated two aspects of the irradiator. The first was to evaluate how well the polyethylene moderates neutrons by simulating the ^{252}Cf source in the irradiator and comparing those results to a baseline calculation assuming that the source was in air. Second, the effectiveness of the borated polyethylene layers to shield workers from neutron and gamma-ray radiation was characterized and compared to measurements at positions outside the irradiator where human contact might be made.

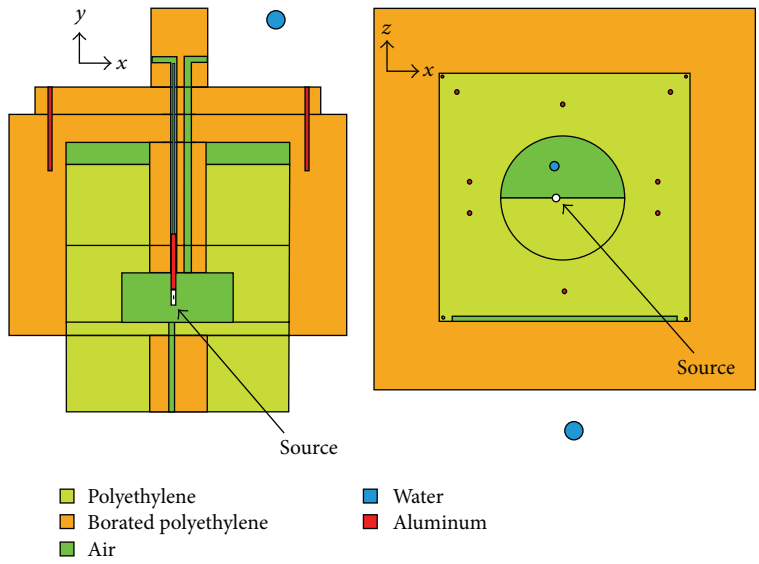

Figure 5: MCNP model of neutron irradiator.

Table 5: Properties of select irradiator materials.

Material	Density (g/cm^3)	Composition (mass fraction)
Cf_2O_3 in Pd matrix	12.02	Pd (0.999); Cf_2O_3 (0.001) with the Cf comprised of ^{252}Cf (0.79); ^{251}Cf (0.04); ^{250}Cf (0.15); ^{249}Cf (0.02)
Source encapsulation	8.03	Stainless steel 304L (1.0)
Pure polyethylene	0.92	H (0.1437); C (0.8563)
Borated polyethylene	0.95	H (0.116); C (0.612); O (0.222); B (0.050)

The Monte Carlo N-Particle (MCNP) transport code [28] was used to characterize neutron and gamma-ray dose rates within the irradiation chamber and at operator contact areas. The neutron irradiator geometry and material compositions were implemented in MCNP5, as shown in Figure 5, although some minor simplifications were made in the model. Examples of these simplifications include neglecting the notches that allow the inner chamber shielding to be gripped, the air gaps which allow the turntable to rotate with little friction, and some trace elements such as nitrogen which are present in the stainless steel source encapsulation.

Neglecting conventional substances such as water, air, and aluminum, Table 5 lists details of the materials used in the MCNP modeling. As noted in Section 2, the californium oxide is in a palladium matrix and the cermet wire is doubly encapsulated. Cf_2O_3 has reported densities of 11.39 to 12.69 g/cm^3 [29] which are similar to the density of Pd. With Pd representing 99.9% of the cermet wire, Pd density is adopted for the Pd-Cf_2O_3 mixture. Older ^{252}Cf sources employed primary and secondary encapsulations of a 90% Pt-10% Rh alloy and Type 304L stainless steel, respectively [30], but the present source uses stainless steel for both. The overall cylindrical source capsule for the 25 μg of ^{252}Cf is 32.6 mm × 9.42 mm diameter. The MCNP simulations were carried out using a thermal scattering cross section library, $S(\alpha, \beta)$, for hydrogen in polyethylene (PE) at 293.6 K for both the pure and borated PE, whose other material properties given in Table 5 were taken from the manufacturer data sheets. Neutrons from (α, n) reactions with oxygen are ignored since Stoddard found those neutron emissions to be insignificant compared to that produced by spontaneous fission [31]. The fluxes and doses are tabulated using standard F4 and F6 cell tallies, respectively.

An average of 3.7675 neutrons [32] and between 7.98 [33] and 10.3 [34] photons are released per ^{252}Cf spontaneous fission. The latter photon value was used in this research as it shows better agreement with the measurements. The neutron spectrum was modeled in MCNP using the built-in Watt fission spectrum for ^{252}Cf, which has the form [35]

$$f(E) = C \exp\left(-\frac{E}{a}\right) \sinh\left(\sqrt{bE}\right), \quad (2)$$

where C is a normalization constant, $a = 1.025$ MeV, $b = 2.926$ MeV^{-1}, and E is the neutron energy in MeV.

The corresponding ^{252}Cf gamma emission spectrum is not provided in MCNP. Consequently, published data were consulted to obtain a photon source description. It was important to consider only those published gamma-ray spectra which provide the actual number of gamma rays being emitted [36] as opposed to "counts" which depends on the detector efficiency [37]. Unfolding a spectrum removes the effect of detector efficiency. Gamma-ray spectra before and

after unfolding are shown, for example, in [37]. Preliminary simulations were performed to compare the MCNP gamma-ray dose rate outputs to manufacturer-given values at 1 m in dry air. It was found that the two spectra reported in 2008 [36], which account for both prompt and delayed gamma rays, produced simulation results which agreed well with physical measurements but were below the manufacturer dose rate by about 10%. Those prompt and delayed gamma-ray spectra are as follows:

$$N_{\text{prompt}}(E) = \begin{cases} 6.6 & 0 < E < 0.5\,\text{MeV} \\ 20.2e^{-1.78E} & 0.5 < E < 1.4\,\text{MeV} \\ 7.2e^{-1.09E} & 1.4 < E < 10.4\,\text{MeV}, \end{cases} \quad (3)$$

$$N_{\text{delayed}}(E) = e^{-1.1E}.$$

To characterize the neutron irradiator performance, MCNP was used to obtain the dose rate to water phantoms located (a) within the inner irradiation chamber, (b) in front of the access door, and (c) near the handlebars where the turntable placement is controlled at the top of the irradiator. None of these locations are shielded by the lead structure. The front and top water phantoms were placed relatively close to the irradiator surface as measurements from a pancake probe are used for simulation verification in the case of gamma rays. Three separate simulations were run to account individually for the delayed and prompt gamma rays, as well as the secondary gamma rays which are emitted as a result of (n, γ) reactions with materials. The delayed and prompt gamma results were multiplied by the gamma-ray emission rate of the ^{252}Cf source to convert from the default dose-per-source-particle to a dose rate while the secondary gamma-ray results were multiplied by the neutron emission rate. These results are reported in Figure 6 (note the different scales used for the access door and handlebars locations). As expected, the gamma-ray dose rate outside the irradiator is much less than that inside. Within the irradiation cavity, the gamma-ray dose from the prompt and delayed components dominate and are approximately equal whereas the exterior dose is comprised near equally of the three components.

The total gamma-ray dose rates obtained in the MCNP simulations were 159 μGy/h (15.9 mrad/h) at the front of the irradiator (within 0.5% of the measurements in Table 4) and 80.6 μGy/h (8.06 mrad/h) for the top (within 2.3%). This agreement verifies the validity of the model. Gamma-ray dose rates were not measured inside of the chamber, but simulations showed the value to be 9.29 mGy/h (929 mrad/h). Because the simulation results were lower than the manufacturer-quoted dose rate, these results may indicate that the manufacturer-quoted dose rate is actually too high. This is plausible because the manufacturer dose rate originates from a 1965 publication [31].

Similar simulations were done in MCNP to characterize the neutron dose rates. The water phantoms were relocated according to the position of the center of the neutron dose rate meter. The MCNP dose values were converted to a unit of rem by applying the neutron quality factors [38] to the halfway points between the stated energy values. The neutron

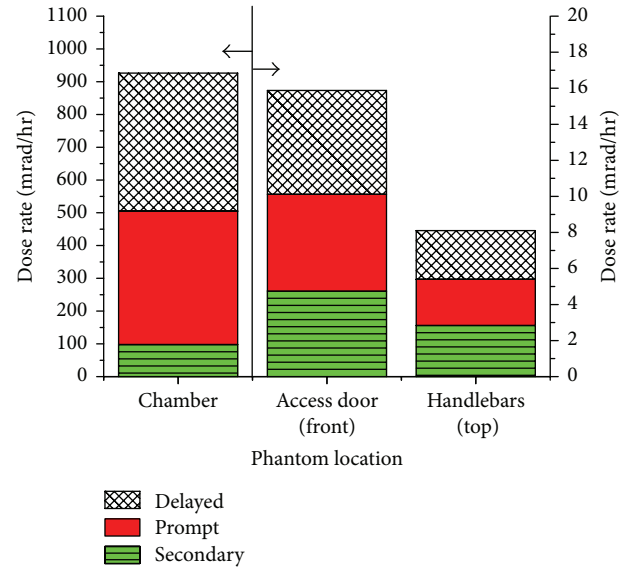

Figure 6: Calculated gamma-ray dose rates to various locations of the irradiator. Note the use of different vertical axes.

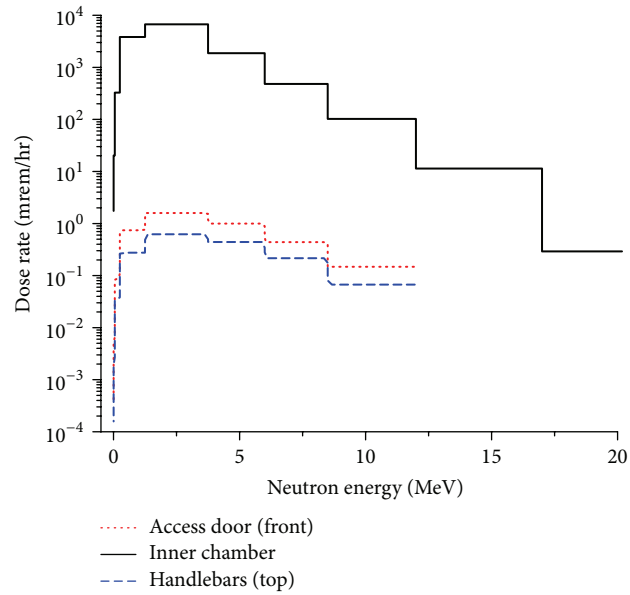

Figure 7: Neutron dose rates to water phantoms at various irradiator locations.

dose rates to three different locations after conversion are shown in Figure 7. The modified dose rates were then summed to obtain the total dose rate. The calculated neutron dose rates at the front and top of the irradiator were 3.9 and 1.9 mrem/h, respectively, compared to measurements of 4.2 and 2.2 mrem/h.

It was found that the neutron dose rate at the top location is sensitive to the vertical position of the ^{252}Cf source within the irradiation cavity since the source comes into closer proximity with the highly shielding borated polyethylene upper extension cylinder. Shifting the ^{252}Cf source 1.27 cm

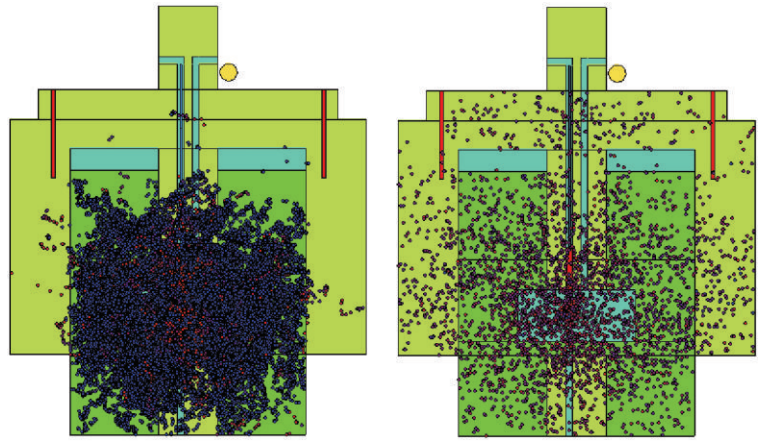

(a) (b)

Figure 8: (a) Neutron and (b) gamma-ray interactions with the irradiator.

(0.5 inches) upward, which is within the resolution of the marker on the source cable, changes the total dose rate by 13%. Between the fluctuation of the analog readout (due to the low dose rate) and the imprecision in placing the ^{252}Cf source in the same exact vertical position from irradiation to irradiation, the MCNP results were shown to agree with 10% of the neutron survey meter measurements which falls within the manufacturer true value margin for the neutron dose rate [39].

The particle fluxes to a water phantom placed inside the irradiation chamber for neutrons and the three sources of gamma rays were computed. The total neutron flux was found to be 3.03×10^5 n/(cm^2·s) while the total gamma-ray flux was $8.02 \times 10^5 \gamma$/(cm^2·s). The particle interactions within the irradiator are shown in Figure 8. As shown in Figure 8(a), neutrons are moderated within the polyethylene layers to increase the neutron flux but are quickly absorbed by the surrounding borated polyethylene shielding. The moderated neutron flux was computed to be 2.9 times the baseline flux in air. The gamma rays shown in Figure 8(b) are not absorbed but the dose rate decreases appreciably, as shown in Figure 6, mostly due to inverse distance squared spreading.

The MCNP computed neutron spectrum within the sample chamber is plotted in Figure 9 in terms of $E\ d\phi/dE$, which is an approximation to neutron lethargy, and normalized to the ^{252}Cf source activity. The graph shows both the spectrum for the as-built configuration using the polyethylene (PE) moderator and results from a separate MCNP run in which the pure and borated PE were replaced by air in the simulation to gauge the impact of the moderator. The thermal (<1 eV) and fast (>1 MeV) fluences comprise 42% and 30% of the total, respectively. The moderated spectrum ensures greater activation of most nuclides, which typically have larger thermal absorption cross sections. The spectrum shown in Figure 9 compares very favorably to recently reported measurements of a ^{252}Cf source shielded by various materials, including polyethylene [40].

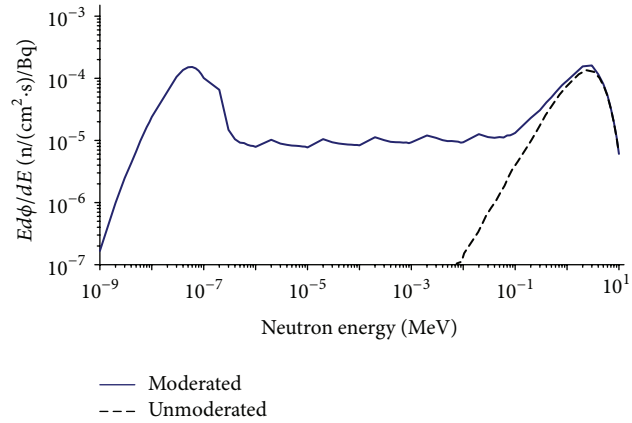

Figure 9: Calculated neutron spectrum within the sample chamber with and without the pure and borated polyethylene present.

5. Conclusions

This neutron source installation was researched, designed, and conducted to provide a modern radioisotopic neutron irradiator. ^{252}Cf has become more affordable over the last few decades due to advances in nuclear technology and isotope production methods. This paper furnishes the scientific community with a guide to constructing an irradiation apparatus. The moderated 25 μg of ^{252}Cf produces a neutron flux of 3×10^5 n/(cm^2·s) to the sample chamber as found with MCNP simulations, with the polyethylene increasing the flux by approximately three times the unmoderated value. The ^{252}Cf-based irradiator measures 0.75 m in diameter and weighs 360 kg. As compared to a research reactor or accelerator occupying significant space, an irradiator such as the one described here can be readily integrated into existing laboratories as well as being easily stored and/or transported between sites. The measured external neutron and gamma-ray dose rates are approximately 30 μSv/h and

120 μGy/h, respectively, during irradiation. MCNP estimates of the gamma-ray and neutron doses were within about 2% and 10% of the measurements, respectively.

Competing Interests

The authors declare that they have no competing interests.

References

[1] M. Trainer, "Neutron activation: an invaluable technique for teaching applied radiation," *European Journal of Physics*, vol. 23, no. 1, pp. 55–60, 2002.

[2] J. Csikai, "Use of small-accelerator and isotope-neutron sources in materials research," in *International Conference on Neutrons and Their Applications*, vol. 2339 of *Proceedings of SPIE*, pp. 318–334, March 1995.

[3] J. Steiner, A. Anderson, and M. De Marco, "Production of ^{239}Pu from a natural Uranium disk and 'hot' rock using a neutron howitzer," http://arxiv.org/abs/0805.3665.

[4] A. M. Osman, A. M. Abdel-Monem, and A. M. Ali, "Optimization of thermal neutron flux in an irradiator assembly with different isotopic sources," *Annals of Nuclear Energy*, vol. 68, pp. 10–14, 2014.

[5] D. M. Fouquet, J. Razvi, and W. L. Whittemore, "TRIGA research reactors: a pathway to the peaceful applications of nuclear energy," *Nuclear News*, vol. 46, no. 12, pp. 46–56, 2003.

[6] R. L. Murray, "Reactor use in nuclear engineering programs," *Nuclear Technology*, vol. 27, no. 1, pp. 15–17, 1975.

[7] J. A. Bernard and L.-W. Hu, "University research reactors: issues and challenges," *Nuclear Technology*, vol. 131, no. 3, pp. 379–384, 2000.

[8] J. A. Bernard and L. W. Hu, "University research reactors: issues and challenges," in *Proceedings of the IEEE Nuclear Science Symposium Conference Record*, pp. 2149–2152, Toronto, Canada, November 1998.

[9] N. Xoubi, "Design, development and installation of jordan subcritical assembly," *Science and Technology of Nuclear Installations*, vol. 2013, Article ID 197502, 5 pages, 2013.

[10] Research Reactor Database, International Atomic Energy Agency, https://nucleus.iaea.org/RRDB/.

[11] US Nuclear Regulatory Commission, *Information Digest, NUREG 1350*, NRC, Washington, DC, USA, 2015.

[12] N. Shugart and J. King, "Neutronic analysis of the geological survey TRIGA reactor," *Annals of Nuclear Energy*, vol. 64, pp. 122–134, 2014.

[13] A. Sinha, T. Roy, Y. Kashyap et al., "BRAHMMA: a compact experimental accelerator driven subcritical facility using D-T/D-D neutron source," *Annals of Nuclear Energy*, vol. 75, pp. 590–594, 2015.

[14] G. Bauwens, A. Noblet, and G. Sylin, "A compact accelerator-type neutron generator," *Journal of Physics E: Scientific Instruments*, vol. 18, pp. 228–231, 1984.

[15] G. Shani, "Activation analysis with isotopic sources," *Activation Analysis*, vol. 2, pp. 239–296, 1990.

[16] Z. R. Harvey, *Neutron flux and energy characterization of a plutonium-beryllium isotopic neutron source by Monte Carlo simulation with verification by neutron activation analysis [M.S. thesis]*, University of Nevada, Las Vegas, Nev, USA, 2010.

[17] R. B. M. Sogbadji, R. G. Abrefah, B. J. B. Nyarko, E. H. K. Akaho, H. C. Odoi, and S. Attakorah-Birinkorang, "The design of a multisource americium-beryllium (Am-Be) neutron irradiation facility using MCNP for the neutronic performance calculation," *Applied Radiation and Isotopes*, vol. 90, pp. 192–196, 2014.

[18] N. Xu, K. Kuhn, D. Gallimore et al., "Elemental composition in sealed plutonium-beryllium neutron sources," *Applied Radiation and Isotopes*, vol. 95, pp. 85–89, 2015.

[19] E. A. Lorch, "Neutron spectra of ^{214}Am/B, ^{241}Am/Be, ^{241}Am/F, ^{242}Cm/Be, ^{238}Pu/^{13}C and ^{252}Cf isotopic neutron sources," *The International Journal of Applied Radiation and Isotopes*, vol. 24, no. 10, pp. 585–591, 1973.

[20] Phoenix Nuclear Labs, http://phoenixnuclearlabs.com/product/high-yield-neutron-generator/.

[21] High Tech Sources, *Californium-252*, QSA Global, Didcot, UK, 2013.

[22] W. C. Mosley, P. E. McBeath, and P. K. Smith, "Californium oxide-palladium cermet wire as a ^{252}Cf neutron source form," Tech. Rep. DP-1320, Savannah River Laboratory, Aiken, SC, USA, 1974.

[23] L. B. Magnusson, M. H. Studier, P. R. Fields et al., "Berkelium and californium isotopes produced in neutron irradiation of plutonium," *Physical Review*, vol. 96, no. 6, pp. 1576–1582, 1954.

[24] J. De La Cova, W. Gilbert, M. Graham et al., "A ^{252}Cf neutron irradiator for testing electronic components for the Large Hadron Collider," in *Proceedings of the IEEE Nuclear Science Symposium Conference Record*, vol. 2, pp. 670–673, IEEE, San Diego, Calif, USA, November 2001.

[25] ATOMIC Accessories, '*Visiflux*' *Neutron Howitzers*, Baird-Atomic, Inc, Cambridge, Mass, USA, http://pbadupws.nrc.gov/docs/ML0515/ML051540354.pdf.

[26] W. S. Rawls and H. G. Voss, "A versatile, inexpensive neutron howitzer," *American Journal of Physics*, vol. 34, no. 12, p. 1182, 1966.

[27] M. Tohamy, M. Fayez-Hassan, S. Abd El-Ghany, S. M. El-Minyawi, M. M. Abd El-Khalik, and M. N. H. Comsan, "A dual-hemisphere irradiation facility for ^{241}Am-Be isotopic neutron source," *Journal of Nuclear and Radiation Physics*, vol. 5, no. 2, pp. 51–58, 2010.

[28] X-5 Monte Carlo Team, *MCNP—A General Monte Carlo N-Particle Transport Code, Version 5. Volume I: Overview and Theory*, LA-UR-03-1987, Los Alamos National Laboratory, 2008.

[29] N. M. Edelstein, J. Fuger, J. J. Katz, and L. R. Morss, "Summary and comparison of properties of the actinide and transactinide elements," in *The Chemistry of the Actinide and Transactinide Elements*, L. R. Morss, N. M. Edelstein, and J. Fuger, Eds., pp. 1753–1835, Springer, Berlin, Germany, 2007.

[30] A. R. Boulogne and J. P. Faraci, "Californium-252 neutron sources for industrial applications," *Nuclear Technology*, vol. 11, no. 1, pp. 75–83, 1971.

[31] D. H. Stoddard, "Radiation properties of californium-252," USAEC Report DP-986, Savannah River Laboratory, Aiken, SC, USA, 1965.

[32] V. Chisté, M.-M. Bé, C. Dulieu et al., "Table of Radionuclides (Vol. 4-A = 133 to 252)," Bureau International Des Poids Et Mesures, Sèvres, France, 2008.

[33] T. E. Valentine, "Evaluation of prompt gamma rays for use in simulating nuclear safeguard measurements," Tech. Rep. ORNL/TM/-1999/300, Oak Ridge National Laboratory, Oak Ridge, Tenn, USA, 1999.

[34] A. B. Smith, P. R. Fields, and A. M. Friedman, "Prompt gamma rays accompanying the spontaneous fission of Cf-252," *Physical Review*, vol. 104, no. 3, pp. 699–702, 1956.

[35] X-5 Monte Carlo Team, "MCNP—a general monte carlo n-particle transport code, version 5. Volume I: overview and theory," Tech. Rep. LA-UR-03-1987, Los Alamos National Laboratory (LANL), Los Alamos, NM, USA, 2008.

[36] R. B. Hayes, "Preliminary benchmarking efforts and MCNP simulation results for homeland security," *Nuclear Technology*, vol. 168, no. 3, pp. 852–857, 2009.

[37] V. V. Verbinski, H. Weber, and R. E. Sund, "Prompt gamma rays from ^{235}U(n,f), ^{239}Pu(n,f), and spontaneous fission of ^{252}Cf," *Physical Review C*, vol. 7, no. 3, pp. 1173–1185, 1973.

[38] United States Nuclear Regulatory Commission, *NRC: 10 CFR 20.1004 Units of Radiation Dose*, 2014, http://www.nrc.gov/reading-rm/doc-collections/cfr/part020/part020-1004.html.

[39] Ludlum Measurements, *Ludlum Model 12-4 Survey Meter with He-3 Neutron Detector*, 2014, http://www.ludlums.com/images/stories/product_manuals/M12-4.pdf.

[40] R. Radev, "Neutron spectra, fluence and dose rates from bare and moderated Cf-252 sources," Tech. Rep. LLNL-TR-688699, Lawrence Livermore National Laboratory, Livermore, Calif, USA, 2016.